
24 Magnetism

S. T. Bramwell

University College London, Department of Chemistry, Christopher Ingold Laboratories, 20 Gordon Street, London, UK WC1H 0AJ

1 Introduction

This year's report is only slightly changed in format from last year's.¹ Section 1 remains a general introduction in which highlights from not only magnetochemistry, but also the rest of magnetism are identified. Section 2 is devoted to a detailed discussion of some special topics and Section 3 describes other work classified by compound type.

In terms of magnetochemistry, one of the highlights of the year is certainly the design and synthesis by Ohkoshi *et al.*² of a magnetic substance with two "compensation" temperatures (in other words the magnetization reverses twice with changing temperature). This has been discussed by Kahn³ and is described further in Section 2.1.

Ferromagnets, both old and new, have also been discussed in *Nature*. In the field of materials science, Mohn has described how the origin of the famous ferromagnetic "invar effect", that has puzzled scientists for a century, has perhaps finally been solved.⁴ The argument is outlined in Section 2.2. Ceperley has written about a remarkable new ferromagnet based on calcium boride CaB₆.⁵ The doping of half a percent lanthanum ions into this diamagnetic substance produces a ferromagnet with an ordering temperature around 600 K; however, further doping destroys this state. The discussion surrounding this unusual substance is summarised in Section 2.3.

Another exotic type of magnet discussed is "spin ice". Harris⁶ describes the first measurement of the zero-point entropy of a spin ice material, Dy₂Ti₂O₇, by workers at Bell Laboratories. These experiments are described further in Section 2.4 on magnetic frustration.

Both *Nature* and *Science* have reported progress in "high- T_c " superconductivity.⁷⁻⁹ Service⁸ has commented on how "charge stripes" might be the key to understanding high- T_c or, alternatively, a false lead. The undoped parents of the cuprate high T_c materials are antiferromagnets. Charge stripes occur when positively charged holes line up in rows to avoid interacting with the antiferromagnetic spins on neighbouring rows of copper atoms. This unusual phenomenon is just one of the mysterious links between superconductivity (not just

high- T_c) and magnetism, so it seems appropriate to include a section on this emerging topic (Section 2.5). However the coverage of high- T_c will be very selective: the field is now so complex that the emergence of a consensus is certainly hampered by the mass of data and sometimes contradictory arguments. This comment could equally apply to the field of “colossal magnetoresistance” (CMR). Developments in this area have been reported in *Nature*.^{10,11} Some selected studies of the CMR manganites and other magnetoresistive materials are described in Section 2.6.

This introductory section is concluded with a brief review of some notable developments in other areas of magnetic research including physics, engineering, biology and geophysics.

It is common for chemistry undergraduates nowadays to perform or witness the levitation of high- T_c superconducting samples above a magnet. Such levitation is a characteristic of a diamagnetic material. A ferromagnet will always “flip” as a consequence of Earnshaw’s theorem which derives from the fact that a magnetic field in free space cannot possess the maximum that is required for stable equilibrium. A diamagnet on the other hand requires a field minimum for levitation, and this does not violate Earnshaw’s theorem. This year Geim and colleagues¹² have found a simple way of levitating a ferromagnet that does not violate the theorem. The trick is to stabilise its equilibrium through the proximity of a diamagnetic substance. The most spectacular demonstration of this is the levitation of a small but strong NdFeB magnet below a powerful superconducting magnet, with the stabilisation applied by a human finger and thumb above and below the levitating material (in other words the magnet levitates between finger and thumb). Magnetic levitation of the more traditional sort has been in the news concerning the design of fusion reactors.¹³ Workers at MIT plan to magnetically levitate a 500 kg Nb₃Sn superconducting ring to produce a “levitated dipole reactor” in which the reacting plasma would be trapped in hot clouds near the magnet. The normal method of trapping the plasma is in magnetic confinement machines called tokamaks.

The creation, manipulation and imaging of magnetic domains are of importance in connection to magnetic recording. Fukumura *et al.*¹⁴ have reported the spontaneous occurrence of “bubble” domains in an inorganic material. These domains (like tiny bubbles of reversed spin) are useful because they are robust against small perturbations and are small; however their creation usually requires a magnetic field. Therefore, the observation by scanning Hall microscopy of close-packed bubble domains at around 70 K in La_{1.4}Sr_{1.6}Mn₂O₇, a material with ferromagnetic layers, is of interest. Hillebrecht¹⁵ has written about the experiments of Dürr *et al.*¹⁶ who have imaged magnetic domains by circular dichroism in X-ray resonant magnetic scattering. Back *et al.*¹⁷ have reported the reversal of domains on an ultrafast time scale. This was achieved by applying 2 ps magnetic field pulses to reverse the magnetization of cobalt films. The possible application to ultrafast recording schemes was suggested. Equally impressive is the experimental determination¹⁸ of the magnetization of a monodomain nanoparticle by the Foucault method of Lorentz microscopy. This method gives higher spatial resolution than micro-SQUIDS or magnetic force microscopy. The direction of magnetization in particles of SmCo₅, Fe₃O₄ and carbon-coated Fe₅₀Co₅₀ as small as 5 nm in diameter was determined.

Our understanding of magnetic orientation in animals is steadily advancing, but the mechanism of magnetoreception in the higher animals is still a subject of debate. One idea is that the geomagnetic field interacts with photoreceptors. This year Deutschlander *et al.*¹⁹ have found additional evidence for this. They showed that the magnetic navigation of newts is strongly dependent on the wavelength of light to which they are exposed.

The recognition that the earth behaves like a huge magnetic dipole is one of the oldest established results in science and has been exploited as an aid to navigation for thousands of years. It is now understood that the main magnetic field originates from electric currents associated with fluid flow in the liquid iron-rich outer core, while the solid inner core serves to stabilise the field by preventing fast relaxation. An intriguing fact is that the field intensity varies on all time scales from seconds to millions of years. The variation on long time scales can only be established from the geological record. This year Guyodo and Valet²⁰ have provided an authoritative update of paleomagnetic intensity data spanning the past 800 000 years, during which time the field polarity was the same as it is now. Significant dips in the field intensity are found to be correlated with directional excursions, which lends support to the hypothesis of Gubbins,²¹ that the excursions occur when the field reverses in the outer core but not the inner core. Langereis²² has explained that the new compilation of data also casts considerable doubt on the idea that the excursions are anything to do with climate change or that the field intensity is connected to the earth's orbit.

On an even grander scale the sun's magnetic field is also produced by convection deep within its interior. It is very weak (about 0.5 mT) but has been reported by Lockwood *et al.*²³ to have more than doubled in the past one hundred years. This change coincides with a doubling of the number of sunspots and a brightening of the sun by about 0.1%. The obvious suggestion is that this might account for global warming. However, Parker²⁴ stresses that as regards climate change, "In our present state of ignorance it is not possible to assess the importance of individual factors". Elsewhere in the solar system, the global distribution of the magnetization of the crust of the planet Mars has been determined by the Mars Global Surveyor.²⁵

2 Special topics

2.1 A magnet with two compensation temperatures

Ferrimagnets have two or more magnetic sublattices, occupied by species with different magnetic moments that interact antiferromagnetically with their neighbours on the other sublattice(s). At low temperature the magnetic moments of the sublattices fail to cancel each other out, resulting in a net magnetization. Over fifty years ago Néel²⁶ considered a general mean field theory for ferrimagnetic substances with two sublattices. He showed that the different temperature dependence of the magnetic moment on each sublattice could lead to a reversal of the direction of the magnetization at a so-called compensation temperature. The garnets furnish a well-known example of this behaviour. Ohkoshi *et al.*² studied chemical systems

based on the “Prussian Blue” analogue $A_3[Cr(CN)_6]$. With $A = Ni$ and Fe one finds ferromagnetic behaviour, while with $A = Mn$ one finds ferrimagnetic behaviour. Ohkoshi *et al.* considered a mean field theory for a ferrimagnet with *four* types of magnetic ion, corresponding to Ni , Fe , Mn and Cr . Only $A-Cr$ interactions were considered and these were scaled to the ordering temperatures of the pure compounds: 67 K (Mn), 72 K (Ni) and 21 K (Fe). The relevant spin values are $S(Ni^{2+}) = 1$, $S(Mn^{2+}) = 5/2$, $S(Fe^{2+}) = 2$ and $S(Cr^{3+}) = 3/2$. It was shown that, in a certain compositional range, the temperature dependence of the magnetization was such as to exhibit two compensation temperatures. The phase $Ni_{0.22}Mn_{0.60}Fe_{0.18}[Cr(CN)_6] \cdot 7.6H_2O$ was prepared by the reaction of $NiCl_2$, $MnCl_2$ and $FeCl_2$ with $K_3[Cr(CN)_6]$ in the correct proportions and shown to indeed reverse its magnetization twice with temperature: at 35 K and 53 K. It will be interesting to see if this approach can be extended to other ferrimagnetic systems.

2.2 Origin of the invar effect

The invar alloys were discovered by Guillaume in 1897 who found that $Ni_{0.35}Fe_{0.65}$ had exceptionally small thermal expansion over a wide temperature range. Guillaume was awarded the Nobel Prize for his work in 1920 (a year before Einstein). The low thermal expansion of the alloys leads not only to their technological importance, but also to a scientific mystery: what is the cause of the anomalous behaviour? Thermal expansion in general simply results from anharmonic atomic vibrations that must exist in the face-centred cubic alloys. However the invar effect goes away if the temperature is raised above the Curie temperature of the alloys, so a magnetic mechanism has always been assumed. Weiss in 1964 (see ref. 4) suggested that the effect could be understood as the competition of a ferromagnetic ground state with an antiferromagnetic excited state of slightly smaller volume. The latter would lie at thermal energies above the ground state and become thermally populated as the temperature is raised, reducing the overall volume of the system to compensate for thermal vibration. However van Schilfgaarde *et al.*²⁷ have demonstrated a slightly different scenario. Their *ab initio* calculations show the existence of a continuous transition from a ferromagnetic ground state at high volumes to a disordered non-collinear magnetic state at low volumes. The natural paramagnetic disordering of the ferromagnetic system as the temperature increases then drives a relaxation of the structure that counteracts the normal thermal expansion.

2.3 Doped calcium boride: an unusual ferromagnet

The cubic hexaborides, MB_6 , of the alkaline earth and rare earth metals have attracted interest for their unusual electronic properties. CaB_6 adopts a crystal structure that can be thought of as a $CsCl$ arrangement of B_6 octahedra and Ca^{2+} ions. It is believed to be a semimetal, with a small overlap of a mainly B-derived valence band with a mainly Ca-derived conduction band. Doping with La is therefore expected to increase metallic behaviour. Young *et al.*²⁸ have reported that samples doped with La are indeed metals, but with remarkable magnetic properties. $Ca_{1-x}La_xB_6$ with

$x = 0.2$ is weakly paramagnetic, but with much lower doping, $x = 0.005$, becomes a weak ferromagnet with a moment of $0.07 \mu_B$ per La and a Curie temperature of 600 K. Exactly the same effect is observed in the Sr and Ba analogues. One possible explanation is ordered defect moments, but a more exciting possibility, as discussed in detail by Ceperley,⁵ is that $\text{Ca}_{0.995}\text{La}_{0.005}\text{B}_6$ is a realisation of a magnetically ordered “electron gas”, first conjectured by Bloch seventy years ago (see ref. 5). In most metallic substances the electron density is sufficiently high ($> 10^{20}$ electrons cm^{-3}) that the electrons move independently and form a “normal Fermi liquid”. However at very low electron concentration ($< 10^{18}$ electrons cm^{-3}) the potential energy overcomes the kinetic energy and the electrons “freeze” onto lattice sites, the so-called Wigner crystal. At intermediate concentrations (10^{18} – 10^{20} electrons cm^{-3}) one obtains a fluid electron gas but with ferromagnetically polarised electrons. However, Zhitomirsky *et al.*²⁹ have proposed an alternative explanation. They argue that the parent compound CaB_6 is an “excitonic insulator”. This state arises because the valence and conduction bands are only weakly overlapping, so that holes in the valence band and electrons in the conduction band behave as a gas of oppositely charged particles. The electron and holes form excitons through coulombic attraction, which may “condense” to form an insulating state. This process is analogous to the Bose-type condensation of Cooper pairs in a superconductor, with the opening of an energy gap, although in the exciton case the result is that the semimetal becomes an insulator. The addition of extra electrons to the excitonic insulator can be shown to give rise to a weak ferromagnetic state, as this is favoured energetically. Whatever the true physics of these intriguing compounds, it is certainly of chemical interest that tiny but accurate doping of a semimetal can lead to such a high temperature ferromagnetic state.

2.4 Frustrated magnetism

The main focus in frustrated magnetism continues to be the pyrochlore lattice, which is frustrated not only as an antiferromagnet, but also as a ferromagnet when single ion anisotropy is present (see ref. 1). In a so-called spin ice material such as $\text{R}_2\text{Ti}_2\text{O}_7$ ($\text{R} = \text{Ho}, \text{Dy}$) the problem of ordering the magnetic moments is identical to the problem of ordering the hydrogen atoms in (cubic) ice. Pauling³⁰ famously described the disordered ground state of the hydrogen atoms in ice and calculated its entropy to be roughly $R \ln(3/2)$ per mole of water molecules. In ice, hydrogen atoms are displaced from the midpoints of the oxygen–oxygen line of contact, so as to form a longer hydrogen bond and a shorter covalent bond. The spin ice model³¹ makes the analogy between hydrogen displacement vectors and magnetic moments. It is realised experimentally in $\text{Ho}_2\text{Ti}_2\text{O}_7$ and $\text{Dy}_2\text{Ti}_2\text{O}_7$ through a combination of cubic single ion anisotropy and overall ferromagnetic coupling. This year Ramirez *et al.*³² have measured the magnetic specific heat C_H of $\text{Dy}_2\text{Ti}_2\text{O}_7$ down to mK temperatures, and integrated C_H/T to give the entropy. At a temperature of 12 K, well above the energy scale of the magnetic coupling, the entropy is assumed to be $R \ln 2$, because the Dy^{3+} ground state is a doublet. The zero-point entropy is then derived by subtracting the experimental entropy difference between 0.2 K and 12 K from this value. The resulting zero-point entropy was found to be $0.5 R \ln(3/2)$

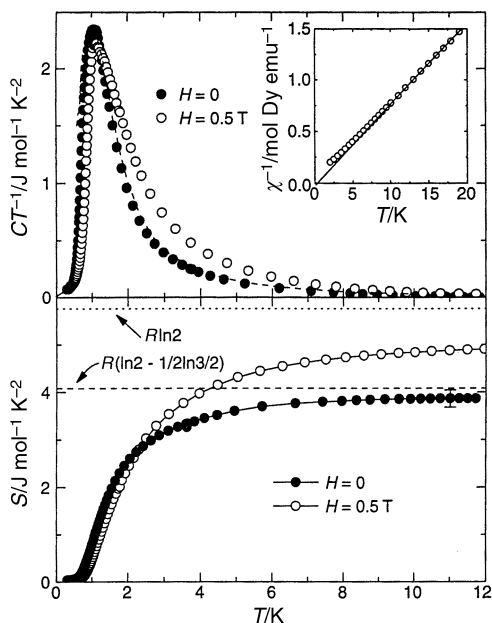


Fig. 1. Specific heat C , entropy S and reciprocal susceptibility $1/\chi$ for spin ice, $\text{Dy}_2\text{Ti}_2\text{O}_7$ (from ref. 32). The entropy change from 0 to 12 K does not reach the $R\ln 2$ expected if the spins are ordered at $T = 0$. Rather, it saturates close to $1/2 R\ln(3/2)$, the zero-point entropy of the ice model.³² In an applied field ($H = 0.5$ T) some of the “missing entropy” is restored.

as expected for spin ice. The measurements are illustrated in Fig. 1. This experiment can be compared to a famous and beautiful experiment of Giauque and Stout, who determined the zero-point entropy of ice by accurately integrating the specific heat up to high temperatures and comparing this with the “spectroscopic” entropy of water in the gas phase.³³

Another rare earth pyrochlore material that has been studied is $\text{Tb}_2\text{Ti}_2\text{O}_7$.³⁴ This has been found to remain a cooperative paramagnet (*i.e.* an interacting system that remains disordered and dynamic) down to 0.07 K. The latter temperature is well below the energy scale of the magnetic coupling between the Tb^{3+} ions (the Curie–Weiss temperature is -19 K). Neutron scattering detects the onset of short range magnetic order at 50 K but the correlation length remains only about 1 lattice spacing down to the lowest temperatures. The magnetic properties of $\text{Tb}_2\text{Ti}_2\text{O}_7$ are rather mysterious and not properly understood; however a competition between near neighbour exchange and anisotropic energy scales seems to be implicated. Other pyrochlore materials under investigation include $\text{R}_2\text{Ru}_2\text{O}_7$ ($\text{R} = \text{Y}, \text{Lu}$) in which the Ru^{4+} ions (d^3) are magnetic. Taira *et al.*³⁵ have re-investigated the magnetic properties of these materials which were previously reported to remain paramagnetic

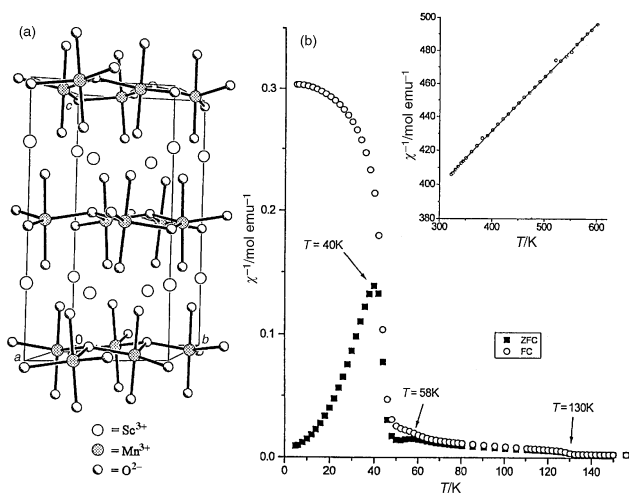


Fig. 2. (a) Crystal structure of ScMnO_3 showing triangular layers of Mn^{3+} (from ref. 37). (b) Direct and reciprocal susceptibility *versus* temperature, showing a Néel temperature at 130 K, a spin reorientation transition near $T = 58$ K, and spin canting transition to weak ferromagnetism at $T = 40$ K.

down to low temperatures. However the comparison of zero-field cooled (ZFC) and field cooled (FC) measurements have revealed a very strong splitting at 80 K. This phenomenon should be investigated further.

The three dimensional geometrically frustrated magnet gadolinium gallium garnet, $\text{Gd}_3\text{Gd}_5\text{O}_{12}$ or “GGG”, forms a spin glass state zero-field in the mK temperature range. With increasing applied field H , the spin glass state gives way eventually to an antiferromagnetic state for $0.7 \leq H \leq 1.4$ T. However, there is an intermediate field range ($H < 0.7$ T) where a “spin liquid” state (another name for a cooperative paramagnet) is thought to occur. Tsui *et al.*³⁶ have used heat capacity, magnetocaloric and thermal conductivity measurements to demonstrate that the spin glass state has a clear upper boundary on the field axis of the magnetic phase diagram between 35 mK and 150 mK. This shows that the transition from spin glass to spin liquid is well defined.

ScMnO_3 , one of a class of Mn materials with the YAIO_3 structure, forms perfectly triangular layers of Mn^{3+} ions in trigonal bipyramidal coordination. The structure and magnetic properties are illustrated in Fig. 2. Bieringer and Greedan³⁷ have measured magnetic susceptibility and neutron diffraction profiles of polycrystalline samples of this material in the range 0–600 K. The antiferromagnetic coupling between the Mn^{3+} spins is very strong, $\theta = -943(7)$ K, and causes magnetic ordering in a non-collinear “120°” structure at 130 K, with ferromagnetic stacking along the c -axis. The same type of ordering is found in RMnO_3 ($R = \text{Ho}–\text{Lu}$). In HoMnO_3 (only) an inplane spin reorientation occurs at temperatures lower than the Néel temperature. ScMnO_3 also shows a spin reorientation transition, in which the angle

of the spins with respect to the crystallographic a -axis changes from about 15° to about 80° between 50 K and 70 K. At higher temperatures, between 80 K and the Néel temperature, 130 K, short range magnetic order was observed with a correlation length ξ roughly constant at $\xi = 13 \text{ \AA}$. At lower temperatures weak ferromagnetism was found to set in as a result of a spin canting transition at $T = 40 \text{ K}$ (see Fig. 2).

Another triangular lattice antiferromagnet of interest is hexagonal UNi_4B . In this material the magnetic U atoms occupy a stacked triangular lattice with antiferromagnetic nearest and next-nearest neighbour coupling within the a - b easy plane and ferromagnetic coupling along the c -axis. However, in this intermetallic material, according to a theory of Lacroix *et al.*³⁸ magnetic frustration is in competition with the Kondo effect (the screening and effective reduction of a paramagnetic moment by conduction electrons). This results in a magnetic transition at 20 K in which only two thirds of the U moments order. Now Movshovich *et al.*³⁹ have used specific heat measurements to detect a further ordering transition at 330 mK, presumably associated with the $1/3$ remaining spins.

As well as being highly relevant to experiment, the Heisenberg antiferromagnet on the triangular lattice is of theoretical interest as a situation where the combination of quantum fluctuations and frustration radically reduces (but does not quite destroy) Néel magnetic order. This year a study by quantum Monte Carlo methods (144 sites) and exact diagonalisation (36 sites) has found that the magnetization at zero temperature is reduced to 41% of its classical value.⁴⁰

2.5 Magnetic origins of superconductivity

A conduction electron in a solid rarely experiences free motion and more typically can be pictured as moving with an associated “cloud” of polarised electronic or nuclear charge. The effective mass of this quasiparticle may sometimes be very large. In the case of the so-called “heavy fermion” compounds it is typically 100 free electron masses. Heavy fermion compounds, usually intermetallics of the lanthanides and actinides, display a strong connection between magnetic and transport properties and there are increasing reports of magnetic-mediated superconductivity in these materials. Thus, Jourdan *et al.*⁴¹ have reported superconductivity mediated by spin fluctuations in the heavy fermion compound UPd_2Al_3 . This compound orders antiferromagnetically at 14.5 K in the bulk and at 12 K in epitaxial films. Superconductivity, coexisting with the antiferromagnetic order, sets in at 2 K. The authors have conducted tunnelling experiments on junctions made from epitaxial UPd_2Al_3 films and shown that the energy scale of the tunneling can most easily be understood in terms of strong coupling between the charge carriers and antiferromagnetic spin fluctuations.

There is a growing body of opinion that the mysterious property of high- T_c superconductivity is also associated with magnetic fluctuations. Lee *et al.*⁴² have discovered more evidence that is consistent with this hypothesis. The copper in lanthanum cuprate is the origin of the antiferromagnetism in the undoped material and of the superconductivity in the doped material. Lee *et al.* (see also ref. 7) have prepared $\text{La}_{1-x}\text{Sr}_x\text{CuO}_4$ single crystals in which the dopants are arranged

periodically, excess oxygen being concentrated in every fourth copper layer. Neutron scattering measurements have shown that an internal magnetic field develops in the sample at the precise temperature at which superconductivity sets in. As well as possibly supporting magnetic mediated superconductivity, it is also possible that there is a spatial segregation of magnetism and superconductivity at a microscopic level in the material. For example, there might be two types of copper atom (near and far from dopants) or segregated holes. On a similar theme, there is increasing evidence of the importance of “charge stripes”⁸ in the cuprate superconductors. These are inherently one-dimensional in contrast to the symmetry of the parent materials (*e.g.* La_2CuO_4) which is quasi-two-dimensional. Experimental evidence for one-dimensional electronic behaviour was observed in $\text{La}_{1.28}\text{Nd}_{0.6}\text{Sr}_{0.12}\text{CuO}_4$ by angle-resolved photoelectron spectroscopy⁴³ and in $\text{La}_{1.4-x}\text{Nd}_{0.6}\text{Sr}_x\text{CuO}_4$ by transport measurements.⁴⁴

To understand the full connection between magnetism and high- T_c superconductivity, a full characterisation of the magnetic properties of the high- T_c materials is vital. In this context, a detailed inelastic neutron scattering study of $\text{YBa}_2\text{Cu}_3\text{O}_{6+x}$ is noted.⁴⁵ The normal state of the “YBCO” materials shows the famous pseudogap in the electronic excitation spectrum. However ^{63}Cu NMR measurements find no dependence of the spin part of this gap on magnetic field from 0–15 T, suggesting that the energy scale of the pseudogap is large compared to the Zeeman energy (20 K).⁴⁶

2.6 Colossal magnetoresistance

In the CMR manganites, charge ordering of Mn^{3+} and Mn^{4+} is known to compete with double exchange, favouring an insulator and metal respectively. The charge ordered states “melt” above a particular temperature to produce a paramagnetic phase in which CMR is particularly strong (see ref. 10 for a discussion). One of this year’s highlights is the discovery by Uehara *et al.*⁴⁷ of percolative phase separation in a mixed valence manganite. The authors study $\text{La}_{5/8-y}\text{Pr}_y\text{Ca}_{3/8}\text{MnO}_3$ ($y = 0\text{--}0.4$). The La-rich members of this series are ferromagnetic metals (FM) and the Pr-rich members are charge ordered insulators (COI) below 210 K. Altering the Pr content changes the “chemical pressure” and the stability of the respective phases. Using electron microscopy the authors have shown that this leads to the coexistence of two segregated phases (COI and FM) on length scales ranging from hundreds of nanometres to micrometres. An applied magnetic field is found to change the relative proportions of the phases and in some cases to cause percolation of the FM part, with associated colossal change in resistance. This sensitivity to perturbation is not unique, having been observed in other materials (see ref. 10), but the microscopic origin is particularly clearly identified in the study of Uehara *et al.* Other evidence for percolation behaviour has been reported by Fäth *et al.*⁴⁸ They conducted STM measurements on $\text{La}_{0.7}\text{Ca}_{0.3}\text{MnO}_3$ at 10 nm resolution to observe the percolation behaviour of insulating paramagnetic and metallic ferromagnetic phases. In the latter material the magnetoresistance becomes large near the magnetic transition at 230 K. In another study, Kimura *et al.*⁴⁹ performed X-ray diffraction, resistivity and magnetization measurements on the phase

$\text{Nd}_{0.5}\text{Ca}_{0.5}\text{MnO}_3$. They described its magnetic behaviour as analogous to the “relaxor ferroelectrics” in which ferroelectric clusters are embedded in a paraelectric matrix.

Uhlenbeck *et al.* have elucidated a complex phase diagram for $\text{La}_{0.875}\text{Sr}_{0.125}\text{MnO}_3$ that illustrates the interplay of magnetism, charge order and structural effects in the manganite materials.⁵⁰ Bulk measurements show that the charge ordering transition at 150 K moves to higher temperature with applied magnetic field, while competing with ferromagnetic and structural transitions. $\text{Nd}_{0.5}\text{Sr}_{0.5}\text{MnO}_3$ also shows a competition of orbital ordered insulating and metallic ferromagnetic states.⁵¹ Below 220 K, this material has $d_{x^2-y^2}$ orbital ordering accompanied by antiferromagnetism. At 150 K d_{z^2} orbital ordering sets in with a structural phase transition. The application of a magnetic field causes the material to revert to a metallic ferromagnetic state. This is accompanied by large negative magnetoresistance and an unexpected volume contraction. The composition $\text{La}_{0.88}\text{Sr}_{0.12}\text{MnO}_3$ has been shown to exhibit a transition between two ferromagnetic states driven by orbital ordering.⁵² This phase is a ferromagnetic metal ordering at 172 K, but becomes a ferromagnetic insulator at the orbital ordering temperature of 145 K. The orbital ordering was detected by resonant X-ray scattering.

Junctions made of $\text{La}_{0.7}\text{Sr}_{0.3}\text{MnO}_3/\text{SrTiO}_3/\text{Co}$ have been shown to display inverse tunneling magnetoresistance.⁵³ This system is analogous to tunnel junctions with two ferromagnetic layers of Ni, Co or Fe separated by an insulator such as Al_2O_3 . The application of a magnetic field changes the angle between the magnetization of the two layers and allows tunneling current to flow. The bulk phase $\text{Nd}_{0.45}\text{Sr}_{0.55}\text{MnO}_3$ has been reported to show a similar “spin valve” effect.⁵⁴ The material adopts a layered structure and orders as a ferromagnetic metal within the layers but an antiferromagnetic insulator from layer to layer. It can therefore be viewed as an infinite stack of spin valves which can be “opened” by applying a magnetic field to align all the layers and facilitate double exchange conductivity. The material shows 10% magnetoresistance (MR) at 12 T and 4.2 K.

Like the perovskite manganites, materials based on the pyrochlore $\text{Ti}_2\text{Mn}_2\text{O}_7$ have been reported to show a connection between magnetoresistance and frozen in magnetic disorder, in this case cluster glass behaviour.⁵⁵ A cluster glass is basically a spin glass formed by frozen magnetic domains. Doping $\text{Ti}_2\text{Mn}_2\text{O}_7$ with bismuth to form $\text{Ti}_{2-x}\text{Bi}_x\text{Mn}_2\text{O}_7$ results in the progressive formation of a cluster glass state, which prevents long range magnetic order for $x \geq 0.2$. At the same time the magnetoresistance increases from 10²⁰% at $x = 0.1$ to 10⁴⁰% at $x = 0.2$. It is suggested that this result indicates the importance of spin polaron conductivity. The sample is a ferromagnetic metal at low doping and a cluster glass at high doping, with a metal-insulator transition temperature that decreases with increasing doping level. The samples ($x = 0-0.5$) were prepared at high pressure in a piston-cylinder press.

Other classes of material are also reported to show colossal magnetoresistance. The perovskite-type material $\text{CaCu}_3\text{Mn}_4\text{O}_{12}$ is a ferromagnet at temperatures below 355 K and shows 40% MR at 20 K in a field of 5 T.⁵⁶ The authors of this work suggest that the material does not have double exchange. Electrodeposited single crystal Bi films show 250% magnetoresistance at 300 K, increasing to 380 000% at 5 K.⁵⁷ This result serves to emphasise the unusual semimetallic properties of elemental bismuth, which relies for conduction on small pockets of the Fermi surface

formed by band overlap. Bismuth has a slightly distorted cubic structure having two electrons per primitive unit cell, so in the absence of band overlap would be a semiconductor. Another unusual substance reported to show giant negative magnetoresistance (70% at 290 K, 0–7 T) is GdI_2 , a ferromagnetic layered d^1 material.⁵⁸

3 Materials

3.1 Borates

A material of great interest characterised this year is $\text{SrCu}_2(\text{BO}_3)_2$.⁵⁹ This has a crystal structure in which closely spaced pairs of copper atoms occupy a rectangular planar lattice. The nearest neighbour distance (within the pair) is only 2.91 Å and there are four next nearest neighbours (in other pairs) at 5.13 Å. Susceptibility measurements show a broad maximum at 15 K with a Curie–Weiss temperature of 95 K. It is suggested that $\text{SrCu}_2(\text{BO}_3)_2$ is a “spin gap” system, or in other words there is a finite quantum mechanical energy gap between the ground state and first excited magnetic state. This is a feature of the simple copper dimers familiar in magnetochemistry; however the theoretical expression for the susceptibility of a pure dimer gives only a poor fit to the susceptibility of $\text{SrCu}_2(\text{BO}_3)_2$. A further interesting observation is that of plateaus in the magnetization-field isotherms at low temperature ($T = 1.7$ and 0.5 K). These correspond to 1/4 and 1/8 of the expected magnetization. Such plateaus are a feature of one-dimensional quantum systems as shown by Oshikawa *et al.*⁶⁰

The theoretical situation in $\text{SrCu}_2(\text{BO}_3)_2$ has been considered in detail by Endoh *et al.*⁵² These authors use exact diagonalisation techniques to demonstrate that $\text{SrCu}_2(\text{BO}_3)_2$ is close to a “quantum critical point” where quantum fluctuations just destroy magnetic order. They define an intradimer coupling J and an interdimer coupling J' and show that a transition from a disordered dimer state to an antiferromagnetically ordered state occurs at $J'/J = 0.7$. The unusual susceptibility behaviour of $\text{SrCu}_2(\text{BO}_3)_2$ is then suggested to result from the fact that J'/J is close to its critical values. The magnetization plateaus are suggested to be related to localised triplet excitations forming a regular lattice structure. It would seem that there is much scope in solid state chemistry for the discovery of other materials which might show similar behaviour.

3.2 Fluorides

Although not widely studied for their magnetic properties, fluorides furnish some of the best available “model magnets” (*i.e.* magnets that approximate statistical mechanical models). This year has seen detailed study of high quality single crystal samples of several such materials.

Rb_2MnF_4 is an excellent realisation of a spin $S = 5/2$ quasi-two-dimensional square-lattice Heisenberg antiferromagnet. However, it has a small easy axis anisotropy (about 1/200 of the near neighbour exchange) arising from dipole–dipole

coupling. The anisotropy puts it into the Ising universality class in zero applied field, with the ordered spins parallel to the c -axis. In general the application of a sufficiently strong longitudinal magnetic field to an Ising-like antiferromagnet results in a spin flop transition, in which the spins turn perpendicular to the field direction and the system passes into the XY universality class. In theory, between these two phases, there is an extremely narrow regime of Heisenberg behaviour which disappears at a bicritical point at $T = 0$. Lehany *et al.*⁶¹ have applied a field along the c -axis to enter the Heisenberg regime and “tune” the uniaxial anisotropy to become as small as possible. In this way they access 2D Heisenberg behaviour to lower temperatures than is possible in zero field. The correlation length ξ was measured by neutron scattering to $\xi > 100$ lattice units, and found to conform to semiclassical theory.

$\text{Fe}_x\text{Zn}_{1-x}\text{F}_2$ has long been used as a model magnet for the study of the random field Ising model. The correspondence occurs because an applied magnetic field results in the magnetic Fe sites experiencing random mean fields made up of the applied field and the random exchange field arising from the dilution. This year a study has been reported in which critical exponents for the phase $\text{Fe}_{0.93}\text{Zn}_{0.07}\text{F}_2$ were measured by neutron scattering, with the result $\nu = 0.87(7)$, $\eta = 0.20$.⁶²

This phase has the advantage over phases of lower magnetic concentration of being able to attain thermodynamic equilibrium.

In LiHoF_4 the Ho^{3+} ions have a doublet ground state with effective spin one half. The compound orders as an Ising ferromagnet at 0.673 K mainly as a result of dipole–dipole coupling. In such a ferromagnetic material “spin flips” can be thought of as events in which the spin rotates like a classical vector, surmounting a potential barrier. In $\text{LiHo}_x\text{Y}_{4-x}\text{F}_4$ however there is the possibility of quantum tunneling of the spins. This can occur spontaneously only in the presence of a transverse field, because in zero field the z -component of the total spin is a conserved quantity. Brooke *et al.*⁶³ have therefore studied $\text{LiHo}_x\text{Y}_{4-x}\text{F}_4$ in a transverse magnetic field as the simplest example of a quantum magnet in which one can compare quantum tunneling and classical relaxation. At about 1 T they observe, using neutron scattering, a transition from a classical ferromagnet to a magnet with history dependent behaviour. The latter is described as a critical, nearly ferromagnetic state. In particular Brooke *et al.* compare the effect of “quantum cooling” (non-zero transverse field) to “classical cooling” (zero transverse field) down to mK temperatures. They find that the quantum cooling results in a state with more rapid fluctuations than that obtained by classical cooling. The advantage of quantum fluctuations in magnetic annealing is suggested to be relevant to optimization problems in general.

3.3 Formates

$\text{Cu}(\text{DCO}_2)_2 \cdot 4\text{D}_2\text{O}$ (CFDT) is probably the best model spin one half Heisenberg antiferromagnet with truly localised spins. This year Rønnow *et al.*⁶⁴ have reported a detailed neutron scattering study of the magnetic correlations in this material and have compared the results with current theories of the two-dimensional quantum Heisenberg antiferromagnet on a square lattice. The latter model is now believed to

have long range magnetic order in the ground state. It has a quasi-classical regime at low temperature, with an exponential growth of the correlation length with J/T where J is the exchange constant (the “CHN” prediction).⁶⁵ At higher temperature ($T > J/2$), a quantum critical regime has been predicted⁶⁶ in which the correlation length varies linearly with J/T . CFDT has $J = 6.3$ meV and orders three-dimensionally at $T_N = 16.5$ K. The Heisenberg behaviour is confined to $T > T_N$. Rønnow *et al.* have determined the correlation length in this regime between $T/J = 0.2$ and $T/J = 1.25$ kT/J. The results show good agreement with the quasi-classical CHN prediction but with a slight deviation towards the quantum critical prediction at higher temperatures.

3.4 Oxides

Early transition metal oxides, particularly those of vanadium, are attracting much attention at present. The spinel LiV_2O_4 is believed to be the first example of a “heavy fermion” compound (see Section 2.5) that is not an f-block alloy. It has an absence of magnetic order or superconductivity down to $T = 0.02$ K, in contrast to LiTi_2O_4 , which is a superconductor ($T_c = 13.7$ K), and ZnV_2O_4 , which is an antiferromagnet ($T_N = 40$ K). Krimmel *et al.*⁶⁷ have provided further neutron scattering evidence for heavy fermion behaviour. The t_{2g} states are split by the low symmetry crystal field to give a low-lying singlet and two excited doublets. The d^1 electrons near the Fermi level occupy the singlet but are strongly hybridised with band states formed by the excited t_{2g} levels. This is a classic recipe for heavy fermion behaviour. Krimmel *et al.* describe LiV_2O_4 as heavy fermion material for $T < 40$ K and a metal close to ferromagnetic order for $T > 40$ K. *Ab initio* electronic structure calculations for LiV_2O_4 have also been reported.⁶⁸

NaV_2O_5 , with a two-leg ladder structure, is the second inorganic compound after CuGeO_3 to be reported to have a “spin Peierls” transition. This is marked by a sharp reduction in the susceptibility below 35 K accompanied by a lattice distortion. However NMR and X-ray studies suggest the transition should properly be seen as a charge ordering transition from $\text{V}^{4.5+}$ to V^{4+} , V^{5+} . Now muon spin relaxation measurements⁶⁹ have detected static spin freezing at $T = 11$ K, that disappears in Na deficient samples. The pyroxene-related spin-chain compound LiVGe_2O_6 also exhibits a spin Peierls transition at 22 K.⁷⁰ Among other vanadium oxides, the exchange interactions and diverse magnetic and electronic properties of the compounds LaV_2O_5 , MgV_2O_5 , CaV_3O_7 and CaV_4O_9 have been discussed on the basis of *ab initio* calculations.⁷¹

The chain like compound $\text{PbNi}_2\text{V}_2\text{O}_8$ (with non-magnetic V^{5+} and magnetic Ni^{2+} , $S = 1$) is described as a new “Haldane gap” antiferromagnet. The Haldane gap is the phenomenon where spin chains with spin $S = \text{integer}$ have a quantum mechanical energy gap to the first excited magnetic state, while those with $S = \text{half integer}$ do not. An $S = 1$ chain therefore does not have a significant magnetic response at low temperature. The ground state singlet is robust and is not destroyed by small perturbations like interchain interactions. However, Uchiyama *et al.*⁷² report that spin vacancies can induce magnetic order in $\text{PbNi}_2\text{V}_2\text{O}_8$. These are introduced by substituting in about 3% Mg which causes an ordering transition at $T =$

3 K, still well below the energy scale of the exchange coupling, $J = 95$ K. The exact mechanism of the ordering transition is not known, but Uchiyama *et al.* suggest that it may be universal. It is likely that free spins liberated by impurity substitution and coupled by the interchain coupling play the crucial role.

Investigations of copper-based oxides are too numerous to mention in detail. However, one notable result described this year is a system which can be “tuned” from a ferromagnetic state to an antiferromagnetic state by chemical substitution.⁷³ The perovskite SeCuO_3 adopts a distorted structure on account of the very small size of the Se^{4+} ion. It is a ferromagnet, ordering at $T_C = 25$ K. However complete replacement of Se by Te results in an antiferromagnet ordering at $T_N = 9$ K. The change is suggested to be due to small changes in bond angles affecting the superexchange pathways. ACuO_3 ($A = \text{Se, Te}$) are made by direct combination of oxides at 900°C under 5.8 GPa pressure in a gold capsule.

3.5 Molecular solids and organic–inorganic complexes

Molecular complexes that exhibit quantum tunneling of the magnetization remain an important subject of investigation (for an introduction see ref. 74). This year, the prototypical compound “ Mn_{12} ” ($\text{Mn}_{12}\text{O}_{12}(\text{CH}_3\text{CO}_2)_{16}(\text{H}_2\text{O}_4)$) has been the subject of an inelastic neutron scattering investigation⁷⁵ of the type discussed in ref. 1. Using the time-of-flight neutron spectrometer IN5 at the Institut Laue-Langevin Grenoble, transitions between different M_S states of the $S = 12$ complex were directly observed. The reader is referred to ref. 75 to see the beautiful energy spectra recorded at 24 K, 14 K and 1.5 K. The accuracy of these spectra allowed a precise determination of the spin Hamiltonian including the crucial transverse field term responsible for quantum tunneling (see also Section 3.3). The latter was deduced to have a magnitude $3.0(5) \times 10^{-5} \text{ cm}^{-1}$.

The “other” important quantum tunneling complex, “ Fe_8 ” ($\{\text{Fe}_8\text{O}_2(\text{OH})_{12}(\text{taccn})_6\}^{8+}$; $\text{taccn} = 1,4,7$ -tetraazacydonorane) has been the subject of a detailed magnetization study.⁷⁶ This complex, with $S = 10$, shows quantum tunneling of the magnetization below 360 mK. In theory, the rate of tunneling depends on the distribution of dipole fields at a site, and so measurement of the short-time magnetic relaxation rate has been used to build up a probability distribution function for the dipole fields.

A new candidate for quantum tunneling of the magnetization has been described by Barra *et al.*⁷⁷ The complex has the formula $[\text{Et}_3\text{NH}]_2[\text{Mn}(\text{CH}_3\text{CN})_4(\text{H}_2\text{O})_2][\text{Mn}_{10}\text{O}_4(\text{biphen})_4\text{Br}_{12}]$ with $\text{biphen} = 2,2'$ -biphenoxide. The energy barrier to spin flips in the spin $S = 12$ Mn_{10} cluster has been estimated to be about 7.7 K. Slow relaxation of the magnetization has been observed below 1 K. However the samples appear to decompose to Mn_3O_4 on aging.

The structural and magnetic properties of $\beta\text{-}[\text{Cu}(\text{dca})_2(\text{pyz})]_n$ ($\text{dca} = \text{dicyanamide}$ ($\text{N}(\text{CN})_2^-$), $\text{pyz} = \text{pyrazine}$) have been described by Jensen *et al.*⁷⁸ This polymeric complex has the structure shown in Fig. 3, and quite strong magnetic coupling, as evidenced by the Curie–Weiss temperature $\theta = -6.2$ K. The magnetic properties appear to be quasi-two-dimensional, but with two types of bridging pathway between the in-plane Cu^{2+} ions.

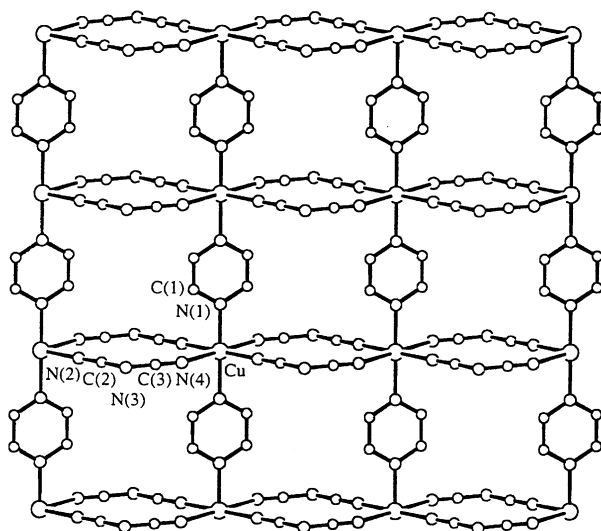


Fig. 3. The sheet structure of β -[Cu(dca)₂(pyz)]_n (from ref. 78).

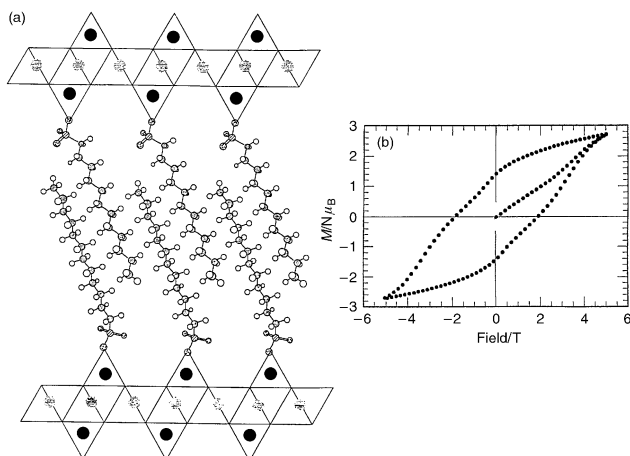


Fig. 4. (a) Idealised triple layer structure of $\text{Co}_5(\text{OH})_8(\text{C}_{12}\text{H}_{25}\text{SO}_3)_2 \cdot 5\text{H}_2\text{O}$, showing a layer of octahedral cobalt sandwiched by two layers of tetrahedral cobalt (from ref. 79). (b) Magnetization *versus* field isotherm at $T = 2$ K showing the properties of a “hard” ferrimagnet.

Finally, we mention a series of organic–inorganic layered hydroxides with diverse magnetic properties.⁷⁹ The layered compounds $\text{Cu}_2(\text{OH})_3(\text{C}_{12}\text{H}_{25}\text{SO}_3) \cdot \text{H}_2\text{O}$, $\text{Ni}_2(\text{OH})_3(\text{C}_{12}\text{H}_{25}\text{SO}_3) \cdot \text{H}_2\text{O}$ and $\text{Co}_5(\text{OH})_8(\text{C}_{12}\text{H}_{25}\text{SO}_3)_2 \cdot 5\text{H}_2\text{O}$ are a paramagnet ($\theta = -38$ K), a ferromagnet ($\theta = +18$ K) and a ferrimagnet ($\theta = -36$ K)

respectively. The interlayer distances in these compounds are typically 25 Å and so one expects them to be two-dimensional. The fact that $\text{Cu}_2(\text{OH})_3(\text{C}_{12}\text{H}_{25}\text{SO}_3)\cdot\text{H}_2\text{O}$ remains paramagnetic down to $T = 2\text{ K}$ might reflect the tendency of a quasi-two-dimensional Heisenberg model to show an ordering temperature that decreases to zero as the interlayer coupling decreases to zero. The analogous Ni compound $\text{Ni}_2(\text{OH})_3(\text{C}_{12}\text{H}_{25}\text{SO}_3)\cdot\text{H}_2\text{O}$ is a ferromagnet ordering at a temperature $T_C = 18\text{ K}$ comparable with the Curie–Weiss constant, while $\text{Co}_5(\text{OH})_8(\text{C}_{12}\text{H}_{25}\text{SO}_3)_2\cdot 5\text{H}_2\text{O}$ is a ferrimagnet that orders magnetically at the surprisingly high temperature of 50 K. The crystal structure and magnetic properties of this interesting compound are illustrated in Fig. 4. It turns out to have a very hard magnetization *versus* field loop at 1.8 K with a coercive field of 19 000 Oe, the largest ever recorded for an organic–metal compound. The hysteresis loop is illustrated in Fig. 4. The slight “stepping” of the curve remains mysterious.

References

- 1 S. T. Bramwell, *Annu. Rep. Prog. Chem., Sect. A*, 1999, **95**, 467.
- 2 S. Ohkoshi, Y. Abe, A. Fujishima and K. Hashimoto, *Phys. Rev. Lett.*, 1999, **82**, 1285.
- 3 O. Khan, *Nature (London)*, 1999, **399**, 21.
- 4 P. Mohn, *Nature (London)*, 1999, **400**, 18.
- 5 D. Ceperley, *Nature (London)*, 1999, **397**, 386.
- 6 M. J. Harris, *Nature (London)*, 1999, **399**, 312.
- 7 A. P. Ramirez, *Nature (London)*, 1999, **399**, 527.
- 8 R. F. Service, *Science*, 1999, **283**, 1109.
- 9 J. Zaanen, *Science*, 1999, **286**, 251.
- 10 P. Littlewood, *Nature (London)*, 1999, **399**, 529.
- 11 N. Mathur, *Nature (London)*, 1999, **400**, 405.
- 12 A. K. Geim, M. D. Simon, M. I. Boumfa and I. O. Heflinger, *Nature (London)*, 1999, **400**, 324.
- 13 J. Riordan, *Science*, 1999, **285**, 823.
- 14 T. Fukumura, H. Suguwara, T. Hasegawa, K. Tanaka, H. Sakuki, T. Kinura and Y. Tokura, *Science*, 1999, **284**, 1969.
- 15 U. Hillebrecht, *Science*, 1999, **284**, 2099.
- 16 H. A. Dürr, E. Dudzik, S. S. Dhesi, J. B. Goodkoop, G. van der Laan, M. Belakhovsky, C. Mocuta, A. Marty and Y. Samson, *Science*, 1999, **284**, 2166.
- 17 C. H. Back, R. Allenspach, W. Weber, S. S. P. Parkin, D. Weller, E. L. Garwin and H. C. Siegmann, *Science*, 1999, **285**, 864.
- 18 S. A. Majetich and Y. Jin, *Science*, 1999, **284**, 470.
- 19 M. E. Deutschlander, S. C. Borland and J. B. Philips, *Nature (London)*, 1999, **400**, 324.
- 20 Y. Guyodo and J.-P. Valet, *Nature (London)*, 1999, **399**, 249.
- 21 D. Gubbins, *Geophys. J. (Oxford)*, 1999, **137**, F1.
- 22 C. G. Langereis, *Nature (London)*, 1999, **399**, 207.
- 23 M. Lockwood, R. Stamper and M. N. Wild, *Nature (London)*, 1999, **399**, 437.
- 24 E. N. Parker, *Nature (London)*, 1999, **399**, 416.
- 25 M. H. Acuña, J. E. P. Connerey, N. F. Ness, R. P. Lin, D. Mitchell, C. N. Carlson, J. McFadden, K. A. Anderson, H. Réme, C. Mazelle, D. Vignes, P. Nasilewski and P. Cloutier, *Science*, 1999, **284**, 791.
- 26 L. Néel, *Ann. Phys.*, 1948, **3**, 137.
- 27 M. van Schilfgaarde, I. A. Abrikosov and B. Johansson, *Nature (London)*, 1999, **400**, 46.
- 28 D. P. Young, D. Hall, M. E. Torelli, Z. Fisk, J. L. Sarrao, J. D. Thompson, H.-R. Ott, S. B. Oseroff, R. G. Goodrich and R. Zysler, *Nature (London)*, 1999, **397**, 412.
- 29 M. E. Zhitomirsky, T. M. Rice and V. L. Anisimov, *Nature (London)*, 1999, **402**, 252.
- 30 L. Pauling, *J. Am. Chem. Soc.*, 1935, **57**, 2680.
- 31 M. J. Harris, S. T. Bramwell, D. F. McMorro, T. Zeiske and K. W. Godfrey, *Phys. Rev. Lett.*, 1997, **79**, 2554.
- 32 A. P. Ramirez, A. Hayashi, R. J. Cava, R. Siddharthan and B. S. Shastry, *Nature (London)*, 1999, **399**, 333.
- 33 W. F. Giaque and J. W. Stout, *J. Am. Chem. Soc.*, 1936, **58**, 1144.

- 34 J. S. Gardner, S. R. Dunsiger, B. D. Gaulin, M. J. P. Gingras, J. E. Greedan, R. F. Kiefl, M. D. Lumsden, W. A. MacFarlane, N. P. Raju, J. E. Sonier, I. P. Swainson and Z. Tun, *Phys. Rev. Lett.*, 1999, **82**, 1012.
- 35 M. Taira, M. Wakeshima and Y. Hinatsu, *J. Solid State Chem.*, 1999, **144**, 216.
- 36 Y. K. Tsui, C. A. Burns, J. Snyder and P. Schiffer, *Phys. Rev. Lett.*, 1999, **82**, 3532.
- 37 M. Bieringer and J. E. Greedan, *J. Solid State Chem.*, 1999, **143**, 123.
- 38 C. Lacroix, B. Canals and M. D. Nuñez-Reguero, *Phys. Rev. Lett.*, 1996, **77**, 5126.
- 39 R. Movshovich, M. Jaine, S. Mentink, A. A. Menovsky and J. A. Mydosh, *Phys. Rev. Lett.*, 1999, **83**, 2065.
- 40 L. Capriotti, A. E. Trumper and S. Sorella, *Phys. Rev. Lett.*, 1999, **82**, 2899.
- 41 M. Jourdan, M. Huth and H. Adrien, *Nature (London)*, 1999, **398**, 47.
- 42 Y. S. Lee, R. J. Birgeneau, M. A. Kastner, Y. Endoh, S. Wakimoto, K. Yamada, R. W. Erwin, S. H. Lee and G. Shirane, *Phys. Rev. B*, 1999, **60**, 3643.
- 43 X. J. Zhou, P. Bogdanov, S. A. Kellar, T. Noda, H. Eisaki, S. Uchida, Z. Hussain and Z.-X. Shen, *Science*, 1999, **286**, 268.
- 44 T. Noda, H. Eisaki and S. Uchida, *Science*, 1999, **286**, 265.
- 45 G. Aeppli, T. G. Perring, R. D. Hunt and F. Dogan, *Science*, 1999, **284**, 1344.
- 46 K. Gorny, O. M. Vyaselev, J. A. Martindale, V. A. Nandor, C. H. Pennington, P. C. Hammel, W. L. Hults, J. L. Smith, P. L. Kuhns, A. P. Reys and W. G. Moulton, *Phys. Rev. Lett.*, 1999, **82**, 1777.
- 47 M. Uehara, S. Mori, C. H. Chen and S.-W. Cheong, *Nature (London)*, 1999, **399**, 560.
- 48 M. Fäth, S. Freisam, A. A. Menovsky, Y. Tomioka, J. Aaris and J. A. Mydosh, *Science*, 1999, **285**, 1540.
- 49 T. Kimura, Y. Tomioka, R. Kumai and Y. Okimoto, *Phys. Rev. Lett.*, 1999, **83**, 3940.
- 50 S. Uhlenbeck, R. Teipen, R. Klingeler, B. Buchner, O. Friedt, M. Hucker, H. Kierspel, T. Niemöller, L. Pinsad, A. Revcolevschi and R. Gross, *Phys. Rev. Lett.*, 1999, **82**, 185.
- 51 R. Mahendiran, M. R. Ibarra, A. Maignan, F. Millange, A. Arulraj, R. Mahesh, B. Raveau and C. N. R. Rao, *Phys. Rev. Lett.*, 1999, **82**, 2191.
- 52 Y. Endoh, K. Hirota, S. Ishihara, S. Okamoto, Y. Murukami, A. Nishizawa, T. Fukuda, H. Kimera, H. Nojiri, K. Kuneke and S. Maekawa, *Phys. Rev. Lett.*, 1999, **82**, 4328.
- 53 J. M. De Teresa, A. Bartelmy, A. Fert, J. P. Contour, R. Lyonnet, F. Montaigne, P. Seneor and A. Vauris, *Phys. Rev. Lett.*, 1999, **82**, 4288.
- 54 H. Kuwahara, T. Okuda, Y. Tomioka, A. Asamitsu and Y. Tokura, *Phys. Rev. Lett.*, 1999, **82**, 4316.
- 55 J. A. Alonso, J. L. Martinez, M. J. Martínez-Lopez, M. T. Casais and M. T. Fernández-Díaz, *Phys. Rev. Lett.*, 1999, **82**, 189.
- 56 Z. Zeng, M. Greenblatt, M. A. Subramanian and M. Croft, *Phys. Rev. Lett.*, 1999, **82**, 3164.
- 57 F. Y. Yang, K. Liu, K. Hong, D. H. Reich, P. C. Season and C. L. Chen, *Science*, 1999, **284**, 1535.
- 58 A. Felser, K. Ahn, R. K. Kremer, R. Seshadri and A. Simon, *J. Solid State Chem.*, 1999, **147**, 19.
- 59 H. Kageyama, Y. Yoshimura, R. Stern, M. V. Mashnikov, K. Onizuka, M. Kato, K. Kosuge, C. P. Slichter and Y. Ueda, *Phys. Rev. Lett.*, 1999, **82**, 3168.
- 60 M. Oshikawa, M. Yamanaka and I. Affleck, *Phys. Rev. Lett.*, 1997, **78**, 1984.
- 61 R. L. Leahy, R. J. Christianson, R. J. Birgeneau and R. W. Erwin, *Phys. Rev. Lett.*, 1999, **82**, 418.
- 62 Z. Slanic, D. P. Belanger and J. A. Fernandez-Baca, *Phys. Rev. Lett.*, 1999, **82**, 426.
- 63 J. Brooke, D. Bitko, T. F. Rosenbaum and G. Aeppli, *Science*, 1999, **284**, 779.
- 64 H. M. Rønnow, D. F. McMorro and A. Harrison, *Phys. Rev. Lett.*, 1999, **82**, 3152.
- 65 S. Chakravarty, B. I. Halperin and D. R. Nelson, *Phys. Rev. Lett.*, 1989, **39**, 2344.
- 66 J. K. Kim and M. Troyer, *Phys. Rev. Lett.*, 1998, **80**, 2705.
- 67 A. Krimmel, A. Loidl, M. Klemm, S. Hom and H. Schober, *Phys. Rev. Lett.*, 1999, **82**, 2919.
- 68 V. I. Anisimov, M. A. Korotin, M. Zöfel, T. Pruschke, K. Le Hur and T. M. Rice, *Phys. Rev. Lett.*, 1999, **83**, 364.
- 69 Y. Fudumoto, K. M. Kojima, M. I. Larkin, G. M. Luke, J. Merrin, B. Nachumi, Y. J. Uemura, M. Isobe and Y. Ueda, *Phys. Rev. Lett.*, 1999, **83**, 3301.
- 70 P. Millet, F. Mila, F. C. Zhang, A. Mambrini, A. B. van Oosten, V. A. Pashchenko, A. Suplice and A. Stepanov, *Phys. Rev. Lett.*, 1999, **83**, 4176.
- 71 M. A. Korotin, J. S. Elfimov, V. I. Anisimov, M. Troyer and D. I. Khomskii, *Phys. Rev. Lett.*, 1999, **83**, 1387.
- 72 Y. Uchiyama, U. Sasago, I. Tsukada, K. Uchinokura, A. Zheludev, T. Hayashi, N. Miura and P. Böni, *Phys. Rev. Lett.*, 1999, **83**, 632.
- 73 M. A. Subramanian, A. P. Ramirez and W. J. Marshall, *Phys. Rev. Lett.*, 1999, **82**, 1558.
- 74 S. T. Bramwell, *Annu. Rep. Prog. Chem., Sect. A.*, 1999, **93**, 457.
- 75 I. Mirebeau, M. Hennion, H. Casalta, A. Andres, H. U. Güdel, A. V. Irodova and A. Caneschi, *Phys. Rev. Lett.*, 1999, **83**, 628.
- 76 W. Wernsdorfer, T. Ohm, S. Sangregorio, R. Sessoli, D. Mailly and C. Paulsen, *Phys. Rev. Lett.*, 1999, **82**, 3905.
- 77 A. L. Barra, A. Caneschi, D. P. Goldberg and R. Sessoli, *J. Solid State Chem.*, 1999, **145**, 484.

- 78 P. Jensen, S. R. Batten, G. D. Fallon, D. C. R. Hockless, B. Moubaraki, K. S. Murray and R. Robson, *J. Solid State Chem.*, 1999, **145**, 387.
- 79 M. Kurmoo, P. Day, A. Derory, C. Estoumès, R. Poinot, M. J. Stead and C. J. Kepert, *J. Solid State Chem.*, 1999, **145**, 452.